Dynamic 3-D shape measurement method based on quadrature transform

Ricardo Legarda-Saenz[1]*, Ramon Rodriguez-Vera[2], and Arturo Espinosa-Romero[1]

[1] *Facultad de Matematicas, Universidad Autonoma de Yucatan. Apdo. Postal 172. 97110 Merida, Yucatan. Mexico*
[2] *Centro de Investigaciones en Optica, A.C. 37000 Leon, Guanajuato. Mexico*

rlegarda@uady.mx

Abstract: In this work, it is presented a combination of temporal phase unwrapping technique and Fourier-based quadrature transform to obtain the dynamic phase map from a vibrating object. The proposed combination results on a very simple algorithm which allows an accurate and versatile 3D reconstruction of the object under analysis.

OCIS codes: (100.2650) Fringe analysis; (100.5070) Phase retrieval; (120.5050) Phase measurement.

References and links

1. F. Chen, G. M. Brown, and M. Song, "Overview of three-dimensional shape measurement using optical methods," Opt. Eng. **39,** 10–22 (2000).
2. E. Stoykova, J. Harizanova, and V. Sainov, "Pattern Projection Profilometry for 3D Coordinates Measurement of Dynamic Scenes," in *Three-Dimensional Television. Capture, Transmission, Display,* H. M. Ozaktas and L. Onural, eds. (Springer, Berlin & Heidelberg, 2008), pp. 85–164.
3. K. J. Gåsvik, *Optical Metrology. Third Edition* (John Wiley & Sons Ltd., Chichester, 2002).
4. X. Su and Q. Zhang, "Dynamic3-D shape measurement method: A review," Opt. Las. Eng. **48,** 191–204 (2010).
5. M. Takeda, H. Ina, and S. Kobayashi, "Fourier-transform method of fringe-pattern analysis for computer-based topography and interferometry, " J. Opt. Soc. Am. **72,** 156–160 (1982).
6. J. M. Huntley and H. Saldner, "Temporal phase-unwrapping algorithm for automated interferogram analysis," Appl. Opt. **32,** 3047–3052 (1993).
7. K. G. Larkin, D. J. Bone, and M. A. Oldfield, "Natural demodulation of two-dimensional fringe patterns. I. General background of the spiral phase quadrature transform," J. Opt. Soc. Am. A **18,** 1862–1870 (2001).
8. M. Servin, J. A. Quiroga, and J. L. Marroquin, "General n-dimensional quadrature transform and its application to interferogram demodulation," J. Opt. Soc. Am. A **20,** 925–934 (2003).
9. T. Kreis, *Holographic Interferometry. Principles and Methods* (Akademie Verlag, Berlin, 1996).
10. B. V. Dorrio and J. L. Fernandez, "Phase-evaluation methods in whole-field optical measurement techniques," Meas. Sci. Technol. **10,** R33–R55 (1999).
11. D. Ghigila and M. D. Pritt, *Two-Dimensional Phase Unwrapping. Theory, Algorithms, and Software*, (John Wiley & Sons Ltd., New York, 1998).
12. S. De Nicola and P. Ferraro, "Fourier transform method of fringe analysis for moire interferometry," J. Opt. A: Pure Appl. Opt. **2,** 228–233 (2000).
13. M. Frigo and S. G. Johnson, "The Design and Implementation of FFTW3," Proc. IEEE **93,** 216–231 (2005).
14. C. Meneses-Fabian, R. Rodriguez-Vera, J. A. Rayas, F. Mendoza-Santoyo, and G. Rodriguez-Zurita, "Surface contour from a low-frequency vibrating object using phase differences and the Fourier-transform method," Opt. Commun. **272,** 310–313 (2007).

1. Introduction

Noncontacting measurement of three-dimensional shape or object profile is important in many areas, including medicine, on-line inspection, computer-aided design-manufacturing and re-

#119528 - $15.00 USD Received 5 Nov 2009; revised 17 Dec 2009; accepted 17 Dec 2009; published 25 Jan 2010

verse engineering. With recent advances in computing technology, some of these techniques have become automated, easier to use in applications and more efficient in data reduction, which has resulted in the development of full-field optical techniques that are being used for real-time profile measurements in a wide range of settings [1, 2].

One important task of real time measurement is the dynamic evaluation. Several optical measurement techniques are used such as fringe projection, holography, moiré interferometry and shearography. In the particular case of fringe projection, early setups were used to observe time-averaged contours; however, these were not suitable to measure the transient deformation of a vibrating object [3]. With the availability of high-speed digital recording, nowadays it is possible to acquire a large sequence of images with the fluctuations of the projected fringe due to the object deformations.

Several approaches can be found in the literature concerning the processing of a large sequence of images [4]. Among them, Fourier transform method [3, 5] is a popular one because of its simplicity: just one fringe pattern is necessary for full-field analysis with high precision. In this method, a fringe pattern with sinusoidal profile is projected onto the object surface; then, the depth information of the object is encoded into a deformed fringe pattern, and it is recorded by an image acquisition sensor. The surface shape can be decoded by calculating Fourier transformation, filtering in spatial frequency domain, and calculating inverse Fourier transformation. However, this method has some limitations; therefore, it can not be used in the automatic processing of large fringe sequences.

In this work, a combination of temporal phase unwrapping technique [6] and Fourier-based quadrature transform [7, 8] are used to obtain the dynamic phase map from a vibrating object, where the aim of the present paper is to present the computational advantages of these techniques. Section 2 describes the proposed method to implement an automatic processing of a sequence of fringe patterns. Section 3 shows the results obtained on the processing of sequences of fringe pattern, and the conclusions are given in Section 4.

2. Theoretical development

The equation which models the observed dynamic fringe pattern can be defined as

$$I(\mathbf{r},t) = a(\mathbf{r}) + b(\mathbf{r},t)\cos[\psi(\mathbf{r},t)] \tag{1}$$

where $\mathbf{r} = (x_1, x_2)$, is a n-dimensional position vector, $a(\mathbf{r})$ is the background illumination, and $b(\mathbf{r},t)$ is the amplitude modulation. One important remark of this equation is that the term $a(\mathbf{r})$ remains constant through the experiment. This means that the intensity of the projection unit in the experimental setup is constant over the measurement, or at least it has slow variations in their intensity.

The phase term $\psi(\mathbf{r},t)$ is defined as

$$\psi(\mathbf{r},t) = \phi(\mathbf{r}) + \varphi(\mathbf{r},t)$$

where the term φ is related to the dynamic object at time t. The conversion from phase to height are given by a transformation

$$z(\mathbf{r}) = \mathscr{T}[\varphi(\mathbf{r},t)]$$

where $\mathscr{T}[\cdot]$ is a function of the geometrical parameters of the experimental setup [3]. The term ϕ is the carrier frequency of the fringe pattern, which is defined as

$$\phi(\mathbf{r}) = \vec{\omega} \cdot f(\mathbf{r})$$

where $\vec{\omega} = (\omega_1, \omega_2)$ is the n-dimensional carrier frequency vector, and $f(\mathbf{r})$ is a function which describes the changes on the carrier frequency due to the experimental setup [3].

#119528 - $15.00 USD Received 5 Nov 2009; revised 17 Dec 2009; accepted 17 Dec 2009; published 25 Jan 2010

A sequence of $N-$frames are taken from the dynamic movement of the object in such a way that

$$\{I(\mathbf{r},t_0), I(\mathbf{r},t_0+\triangle t), I(\mathbf{r},t_0+2\triangle t), \ldots, I(\mathbf{r},t_0+[N-1]\triangle t)\}$$

where $\triangle t$ is the temporal period of the captured frame and is smaller than the temporal period of the vibration cycle. Under this condition, every frame can be seen as

$$I_k(\mathbf{r}) = a(\mathbf{r}) + b_k(\mathbf{r})\cos[\psi_k(\mathbf{r})] \tag{2}$$

where

$$\begin{array}{rcl} I_k(\mathbf{r}) & = & I(\mathbf{r},t_0+k\triangle t) \\ b_k(\mathbf{r}) & = & b(\mathbf{r},t_0+k\triangle t) \\ \psi_k(\mathbf{r}) & = & \psi(\mathbf{r},t_0+k\triangle t) \end{array}$$

for $k = 0,1,\ldots,N-1$.

The demodulation process of a single fringe pattern defined like Eq. (2) is well-known: the Fourier transform of the fringe pattern is computed, then the phase information is isolated by filtering in the frequency plane, and finally the phase is recovered by computing the inverse Fourier transform [3, 5]. To have this method working, the spatial variations of the frequency must be smooth compared to the carrier frequency, and the information in the frequency space has to be well separated [3].

2.1. The general n-dimensional quadrature transform

The conditions imposed at the Fourier-based demodulation method do not allow to implement an automatic demodulation of a sequence of fringe patterns because it is not possible to use the same filtering function for every acquired fringe pattern due to the different variations of the object [2, 9, 10]. Instead, one has to select the appropriate filter to isolate the desired frequency information for each fringe pattern and consequently, the processing of a sequence of patterns using Fourier methods will be manual, becoming a time-consuming and error-prone process.

An alternative to these problems is to estimate the quadrature term of every fringe patterns [7, 8]. First, it is assumed that the background illumination $a(\mathbf{r})$ is filtered from the fringe pattern defined in Eq. (2), resulting in the following fringe pattern [9]

$$g_k(\mathbf{r}) = b_k(\mathbf{r})\cos[\psi_k(\mathbf{r})] \tag{3}$$

The quadrature estimation consists of transforming the fringe pattern shown in Eq. (3) into its quadrature term defined by

$$\hat{g_k}(\mathbf{r}) = -b_k(\mathbf{r})\sin[\psi_k(\mathbf{r})],$$

and obtaining the following fringe complex pattern

$$g_k - i\,\hat{g_k}(\mathbf{r}) = b_k(\mathbf{r})\exp[i\,\psi_k(\mathbf{r})] \tag{4}$$

where $i = \sqrt{-1}$.

The n-dimensional quadrature transform for fringe patterns with carrier frequency is defined as [8]

$$\begin{array}{rl} Q_n\{g_k(\mathbf{r})\} & = -b_k(\mathbf{r})\sin[\psi_k(\mathbf{r})] \\ & = \mathscr{F}^{-1}\left\{-i\,\dfrac{\vec{\omega}\cdot\mathbf{q}}{|\vec{\omega}\cdot\mathbf{q}|}\mathscr{F}\{g_k(\mathbf{r})\}\right\} \end{array} \tag{5}$$

where $\mathbf{q} = (u_1,u_2,\ldots,u_n)$ is the n-dimensional position vector on frequency domain, and $\mathscr{F}\{\cdot\}$ denotes Fourier transform. As it can be observed in this equation, the orientation of the carrier

#119528 - $15.00 USD Received 5 Nov 2009; revised 17 Dec 2009; accepted 17 Dec 2009; published 25 Jan 2010

frequency is the only input parameter necessary to apply the quadrature transform, and this parameter can be obtained from the experimental setup or it can be estimated easily.

Using Eq. (5), we can write the complex fringe pattern shown in Eq. (4) as

$$b_k(\mathbf{r})\exp\left[i\,\psi_k(\mathbf{r})\right] = g_k(\mathbf{r}) - i\,\mathscr{F}^{-1}\left\{-i\,\frac{\vec{\omega}\cdot\mathbf{q}}{|\vec{\omega}\cdot\mathbf{q}|}\mathscr{F}\left\{g_k(\mathbf{r})\right\}\right\} \tag{6}$$

Once the quadrature term was computed using Eq. (5), the wrapped phase is obtained with

$$\hat{\psi}_k(\mathbf{r}) = W\left\{\psi_k\right\} = \arctan\left(\frac{-Q_n\left\{g_k(\mathbf{r})\right\}}{g_k}\right) \tag{7}$$

where W is the wrapping operator [11].

In addition to the well-known computation advantages of the discrete Fourier transform, the quadrature transform shown in Eq. (5) has two significant features: One is the possibility of using an rough estimation of the carrier-frequency orientation because the errors in this term cause only second-order errors on the demodulated phase [7]. The second feature is the demodulation of the fringe pattern without any ad-hoc designed filtering process, avoiding the supervision and design of explicit demodulation-filter for each fringe pattern.

Both features result an important advantage used to implement the proposed automatic processing of a sequence of fringe patterns: every frame acquired in the experiment is demodulated using Eq. 6) given a rough estimation of the carrier-frequency orientation, and the resultant phase is obtained without using the same process mentioned at the beginning of this subsection; i. e. the phase term is demodulated without pointing out any specific location in the frequency domain, reducing errors due to the filtering process.

2.2. Temporal Phase Unwrapping

Once the fringe patterns are demodulated using the quadrature transform, Eqs. (6) and (7), the transient phase change occurring over time can be retrieved by unwrapping the phase maps. The unwrapped phase map $\varphi_M(\mathbf{r})$ can be computed by the sum of the $M-1$ phase differences using the following equation [6, 12]

$$\varphi_M(\mathbf{r}) = \sum_{k=1}^{M} \arctan\left[\frac{\cos\hat{\psi}_k \sin\hat{\psi}_{k-1} - \sin\hat{\psi}_k \cos\hat{\psi}_{k-1}}{\cos\hat{\psi}_k \cos\hat{\psi}_{k-1} + \sin\hat{\psi}_k \sin\hat{\psi}_{k-1}}\right] \tag{8}$$

As it noted, the unwrapping procedure becomes very simple. In addition, one significant advantage of the above procedure is that the carrier frequency and the systematic experimental setup errors are removed from the dynamic phase information. The resultant phase map can be related to the displacement of the dynamic object using a transformation given by the relationship between the phase map and the geometrical parameters of the experimental setup at each point [2, 3].

3. Experimental results

The proposed combination of temporal phase unwrapping technique and quadrature transform used to process the sequence of frames are shown in Algorithm 1. To show the performance of the above algorithm, two sequences of fringe patterns were processed in a 1.8 GHz Pentium Dual Core PC with 8 GBytes of main memory using Ubuntu 9.04 as operative system. The algorithm used to compute the discrete Fourier transform was the FFTW library [13]; in addition, no computational optimization we made in the implementation of Algorithm 1.

#119528 - $15.00 USD Received 5 Nov 2009; revised 17 Dec 2009; accepted 17 Dec 2009; published 25 Jan 2010

Algorithm 1: Retrieval of the dynamic phase $\phi(\mathbf{r}, t_0 + k\triangle t)$

Data: The carrier frequency direction $\vec{\omega}$ and the background term $a(\mathbf{r})$

$k \leftarrow 0$

while *a frame exists in the camera or in files* **do**

read k-frame

$\mathfrak{F}\{g_k\} \leftarrow$ `DC Filter` $[\mathfrak{F}\{I_k\}, \mathfrak{F}\{a(\mathbf{r})\}]$

$\hat{\psi}_k \leftarrow \arctan[-Q_n\{g_k\}, g_k]$; `// Equation (7)`

if $k \geq 1$ **then** $\phi_k(\mathbf{r}) \leftarrow$ `TempPhaseUnwrap` $[\hat{\psi}_k, \hat{\psi}_{k-1}]$; `// Equation (8)`
else $\phi_k(\mathbf{r}) \leftarrow 0$

$k \leftarrow k+1$

end

The first experiment was the processing of a sequence of 100 synthetic frames with resolution of 256 x 256 pixels, where the dynamic phase was defined as

$$\varphi_k(\mathbf{r}) = \kappa \, \sin\left(\frac{2\pi \, k}{25}\right) \, x_1 \, \exp\left[\frac{-(x_1^2 + x_2^2)^{1/2}}{2\sigma^2}\right]. \tag{9}$$

The values of the terms κ and σ are selected arbitrarily to create the desired phase variation. Examples of the fringe patterns generated by Eq. (9) and their resultant demodulated phase maps using Eq. (7) are shown in Fig. 1. The resultant dynamic phase map and the differences between the estimated phase map and the phase given by Eq. (9) are shown in Fig. 2, where it can be observed the very low error obtained with the proposed algorithm. The frame rate obtained to process this sequence was about 6 frames per second.

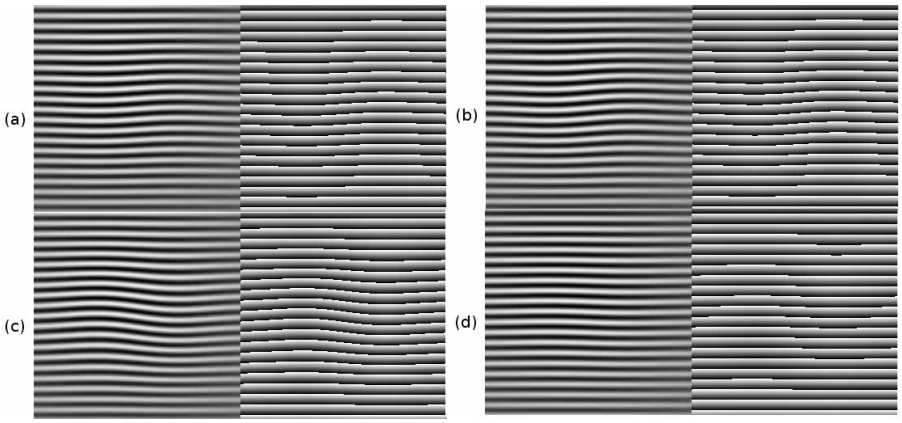

Fig. 1. Examples of the fringe patterns generated by Eq. (9) and their resultant demodulated phase maps using Eq. (7): (a) k = 2, (b) k = 10, (c) k = 18, and (d) k = 24. The complete sequence can be found here (Media 1).

The second experiment was the processing of a sequence of 400 frames with resolution of 640 x 64 pixels, taken from an vibrating cantilever [14]. Examples of the acquired fringe patterns and their resultant demodulated phase maps using Eq. (7) are shown in Fig. 3. The

#119528 - $15.00 USD Received 5 Nov 2009; revised 17 Dec 2009; accepted 17 Dec 2009; published 25 Jan 2010

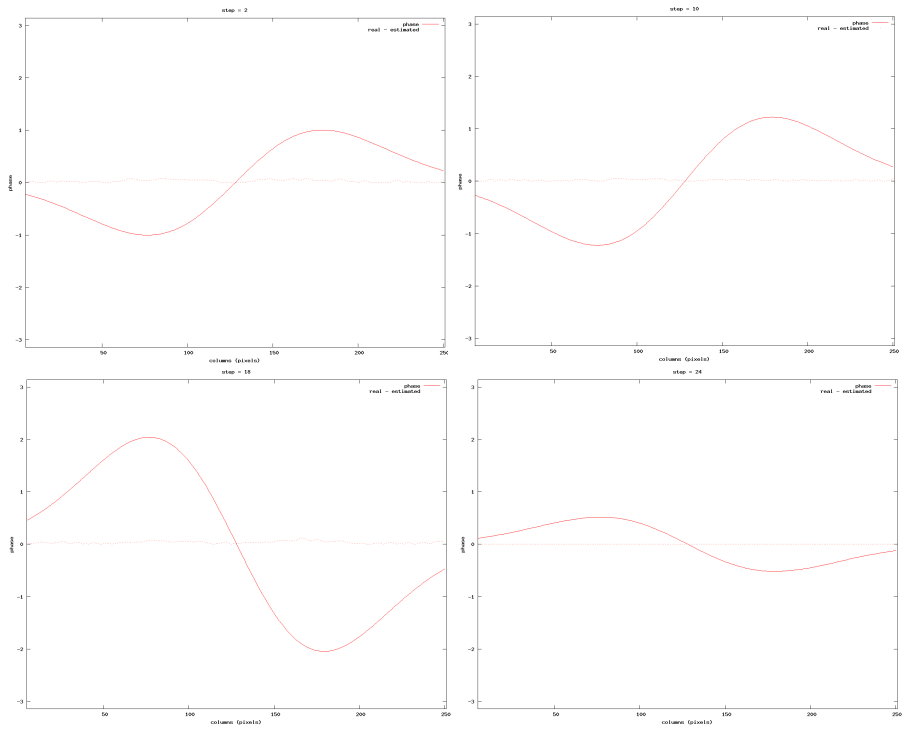

Fig. 2. Middle row of the estimated phase maps computed with Eq. (8) from the phase maps shown in Fig. 1 and the differences found with the real phase map. The complete sequence can be found here (Media 2).

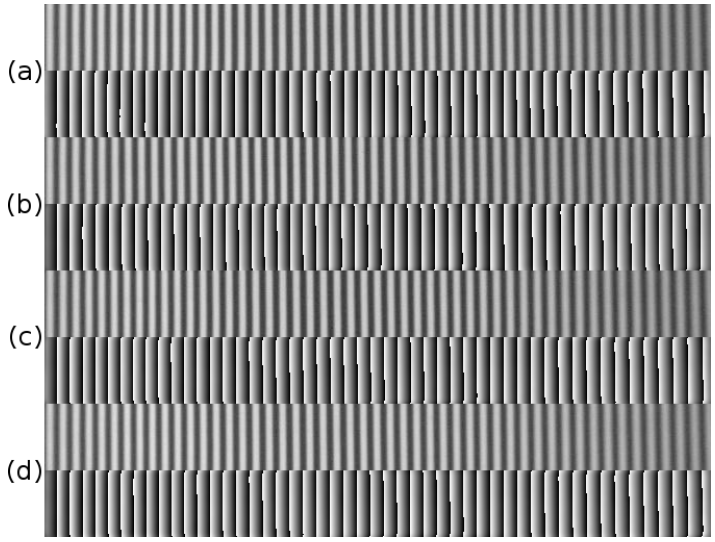

Fig. 3. Examples of the fringe patterns acquired from the experiment and their resultant demodulated phase maps using Eq. (7): (a) k = 3, (b) k = 12, (c) k = 20, and (d) k = 28. The complete sequence can be found here (Media 3).

#119528 - $15.00 USD Received 5 Nov 2009; revised 17 Dec 2009; accepted 17 Dec 2009; published 25 Jan 2010

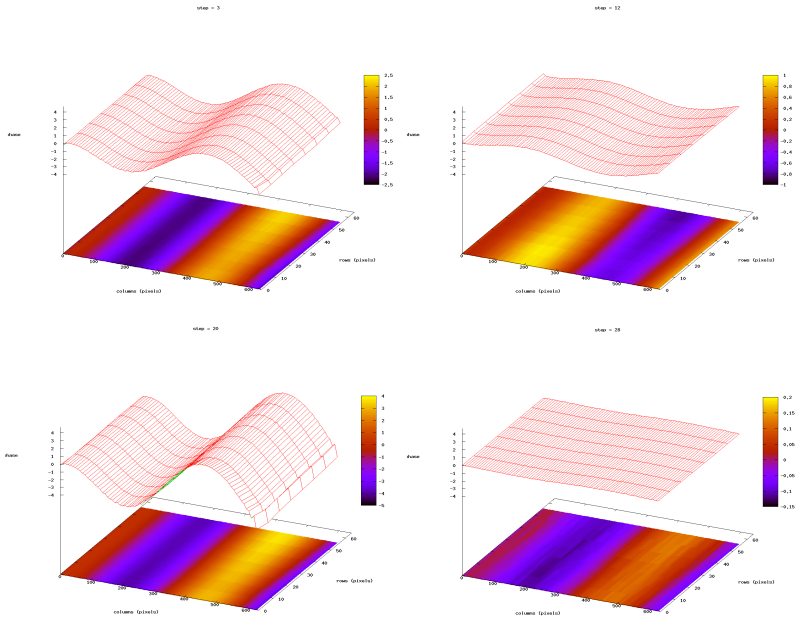

Fig. 4. Estimated phase maps computed with Eq. (8) from the phase maps shown in Fig. 3. The complete sequence can be found here (Media 4).

resultant dynamic phase map are shown in Fig. 4. As it can be compared with the results shown in Ref. [14], the estimated phase maps are consistent with the reported phase maps. The frame rate obtained to process this sequence was about 16 frames per second.

4. Conclusions

In this work, it is presented a combination of temporal phase unwrapping technique and Fourier-based quadrature transform to obtain the dynamic phase map of a vibrating object. The proposed combination results on a very simple algorithm, as it can be observed in Algorithm 1, which allows an accurate and versatile 3D reconstruction of the object under analysis, and it is based on simple and computational efficient techniques. An extra advantage of the proposed method is its feasibility to be implemented on a dedicated hardware for processing in real-time, which is the aim of future research.

Acknowledgments

R. Legarda-Saenz was supported by Consejo Nacional de Ciencia yTecnología (Mexico) under grant 25793-CB-2005-01-49753.

#119528 - $15.00 USD Received 5 Nov 2009; revised 17 Dec 2009; accepted 17 Dec 2009; published 25 Jan 2010